



The large footprint of small-scale artisanal gold mining in Ghana

Abigail Barenblitt^{a,c,*}, Amanda Payton^b, David Lagomasino^b, Lola Fatoyinbo^c, Kofi Asare^d, Kenneth Aidoo^d, Hugo Pigott^e, Charles Kofi Som^e, Laurent Smeets^e, Omar Seidu^e, Danielle Wood^f

^a Earth System Science Interdisciplinary Center, University of Maryland, College Park, MD, United States

^b Department of Coastal Studies, East Carolina University, Wanchese, NC, United States

^c Biospheric Sciences Laboratory, NASA Goddard Space Flight Center, Greenbelt, MD, United States

^d Ghana Space Science and Technology Institute, Accra, Ghana

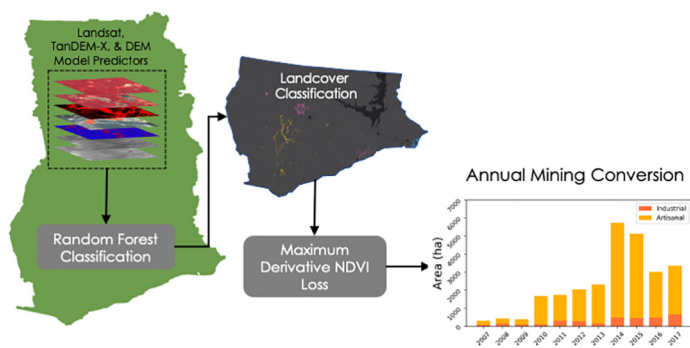
^e Ghana Statistical Service, Accra, Ghana

^f Space Enabled Research Group, Massachusetts Institute of Technology, Cambridge, MA, United States

HIGHLIGHTS

- Land conversion in due to artisanal gold mining = that of urban expansion.
- New mining extent (2005 and 2019) was dominated by artisanal mining (~89%).
- Over 700 ha of artisanal mining was detected in protected areas.
- This mining is degrading and destroying forested ecosystems.

GRAPHICAL ABSTRACT



ARTICLE INFO

Article history:

Received 22 December 2020

Received in revised form 17 March 2021

Accepted 17 March 2021

Available online 22 March 2021

Editor: Mae Sexauer Gustin

Keywords:

Galamsey

Landsat

Extent mapping

NDVI

Google Earth Engine

ABSTRACT

Gold mining has played a significant role in Ghana's economy for centuries. Regulation of this industry has varied over time and while industrial mining is prevalent in the country, the expansion of artisanal mining, or *Galamsey* has escalated in recent years. Many of these artisanal mines are not only harmful to human health due to the use of Mercury (Hg) in the amalgamation process, but also leave a significant footprint on terrestrial ecosystems, degrading and destroying forested ecosystems in the region. In this study, the Landsat image archive available through Google Earth Engine was used to quantify the total footprint of vegetation loss due to artisanal gold mines in Ghana from 2005 to 2019 and understand how conversion of forested regions to mining has changed over a decadal period from 2007 to 2017. A combination of machine learning and change detection algorithms were used to calculate different land cover conversions and the timing of conversion annually. Within the study area of southwestern Ghana, our results indicate that approximately 47,000 ha (± 2218 ha) of vegetation were converted to mining at an average rate of ~ 2600 ha yr^{-1} . The results indicate that a high percentage ($\sim 50\%$) of this mining occurred between 2014 and 2017. Around 700 ha of this mining occurred within protected areas as mapped by the World Database of Protected Areas. In addition to deforestation, increased artisanal mining activity in recent years has the potential to affect human health, access to drinking water resources and food security. This work expands upon limited research into the spatial footprint of *Galamsey* in Ghana, complements mapping efforts by local geographers, and will support efforts by the government of Ghana to monitor deforestation caused by artisanal mining.

© 2021 The Authors. Published by Elsevier B.V. This is an open access article under the CC BY license (<http://creativecommons.org/licenses/by/4.0/>).

* Corresponding author at: 8800 Greenbelt Rd, Greenbelt, MD 20771, United States.

E-mail address: abigail.barenblitt@nasa.gov (A. Barenblitt).

1. Introduction

Precious metals like gold have been a part of local economies for thousands of years and globally remain a highly valued commodity. In Ghana, gold mining is conducted by way of industrial-scale mines, as well as smaller artisanal mines, locally known as *Galamsey*. While this industry has provided economic benefits to local communities, the environmental and health impacts of this industry can be devastating (Hilson, 2002). Exploration and extraction of surface mining requires deforestation, land-clearing, and excavation (Hilson, 2002). Without proper information, exploration methods often lead to the disturbance of landscapes that do not even contain gold (Hilson, 2002). After exploitation, artisanal gold mines are often abandoned with little effort to remediate, making it difficult for forest regrowth or other development to occur (Hilson, 2002). As a result, artisanal and industrial gold mining has been detected as the dominant driver of deforestation in regions like the Ankobra River Basin in South-western Ghana (Obodai et al., 2019).

West Africa is particularly positioned to be a part of this industry as it is the location of four major gold deposits located in geologic shear-zones (Milési et al., 1991). In Ghana alone, these belts cover one-sixth of the country, which has allowed Ghana to produce 70% of sub-Saharan gold (Hilson, 2002) and become the 7th largest producer of gold worldwide (Authority on Gold, 2020). This gold production is separated between artisanal and industrial operations, and since 2012 artisanal mines have accounted for over 30% of Ghana's gold production (Hilson, 2017). This is an increase from 1990 when artisanal mining accounted for less than 5% of gold production (Owusu et al., 2019).

While industrial mining typically occurs within large open pits, artisanal mining is usually superficial and creates swathes of deforested lands and mercury-contaminated sites (Espejo et al., 2018; Swenson et al., 2011). Examples from Papua, Indonesia, and around the world indicate that open-pit mining, such as that employed for artisanal gold mining, can result in excessive mine tailings and runoff (Alonzo et al., 2016; Esdaile and Chalker, 2018; Lobo et al., 2015). These in turn can cause forest inundation and water degradation in areas surrounding mines. Around industrial mines, such as the open-pit Grasberg mine in Papua, forest loss can be >42 times larger than the mine itself (Alonzo et al., 2016). Whereas artisanal open-pit mine tailings leach mercury and increase siltation and suspended particles in waterways (Esdaile and Chalker, 2018; Lobo et al., 2015).

As an adopter of the United Nations Sustainable Development Goals (SDG), Ghana is making efforts to reduce the impact of mining activities. SDGs are an initiative of the United Nations, which aim to end poverty, combat climate change, and reduce environmental degradation by working to reach specific targets that are informed by regular surveys. SDG Targets and Indicators serve as a framework for monitoring conservation needs and successes. For Ghana, addressing artisanal mining is a key objective for achieving several SDGs and the ability to accurately quantify artisanal mining plays a critical role (Government of Ghana, 2019). The cumulative effect of gold mining has the potential to impact a number of SDG Targets and Indicators. Deforestation due to artisanal mining has a clear impact on SDG 15, Life on Land, especially Target 15.1 "By 2020, ensure the conservation, restoration and sustainable use of terrestrial and inland freshwater ecosystems and their services, in particular forests, wetlands, mountains and drylands, in line with obligations under international agreements". Studies of gold mining in other countries have demonstrated that despite being smaller, artisanal mines can still have huge environmental impacts. For example, in Rio Madre de Dios in Brazil, artisanal gold mining has removed 68,228–95,750 ha of forest at a rate of 4437–7432 ha yr⁻¹ since 2000 (Asner and Tupayachi, 2017; Espejo et al., 2018). As a result, even small-scale mines can threaten biodiversity on a larger scale through the removal or pollution of habitat in otherwise diverse regions (Asner and Tupayachi, 2017; Cabeza et al., 2019).

Additional attributes of artisanal mining operations have the potential to impact SDG 3, or Good Health and Wellbeing, SDG 6, or Clean Water

and Sanitation, and SDG2, or Zero Hunger. The process used to separate small gains of gold from sediment, referred to as amalgamation, uses mercury (Hg), which combines with the gold extracted gold to form an amalgam alloy. This amalgamation is then heated to evaporate Hg from the alloy. In order to separate the gold from sediment, the amalgam of gold and Hg is heated. The Hg evaporates and leaves the gold behind because it has a higher melting point. In consequence, the Hg is inhaled and also settles in the soil and nearby water sources. Artisanal mining is currently the largest man-made source of Hg worldwide (UN Environment, 2019). The release of Hg can have serious impacts on human health, including neurological disorders, kidney dysfunction and other disorders (Gibb and O'Leary, 2014). Moreover, the diversion of rivers and spread of artisanal mining into previously arable land can limit access to clean water and put countries at risk of food and water insecurity by valuing minerals over agricultural production (Gilbert and Albert, 2016). This results in a compounded negative impact to health, safety, and food security in local communities.

Even though industrial mines and some artisanal mines may be regulated within the country, they can still have impacts on local communities, as well as coastal communities downstream of the mines (Alonzo et al., 2016). Additionally, artisanal mines were unregulated until the Small Scale Gold Mining Law was enacted in 1989, but regulation remains a challenge (Eshun and Okyere, 2017). Continued difficulty of regulation in the artisanal gold mining industry exacerbates the environmental and health impacts by allowing excess exploration, mercury use, soil and slope destabilization, and carbon emissions, as well as limited remediation of abandoned mining areas (Csillik and Asner, 2020; Diringier et al., 2019; Martinez et al., 2018).

While lack of regulation is a contributing factor to the destructive nature of artisanal mines (Afriyie et al., 2016), obstacles to collecting ground-based information limits our understanding of the impact of Ghana's artisanal mines. Surveying artisanal mines with ground-based techniques can be costly and time-consuming, making it difficult to characterize continually shifting patterns across a region. To capture the spatial footprint of artisanal mines, satellite technology offers the ability to identify patterns across a region at a more appropriate scale (Marceau and Hay, 1999). Satellite observations are already being used to monitor SDGs (Hakimdavar et al., 2020), protected areas (Asner and Tupayachi, 2017; Farrington, 2005), and human health (Anenberg et al., 2020). Cloudy regions can be challenging areas to collect meaningful satellite imagery, but access to archival data and novel analysis techniques can prove incredibly useful for improving our understanding of the impact of artisanal mining in these regions (Alonzo et al., 2016; Isidro et al., 2017; Lobo et al., 2018; Mondal et al., 2019). Previous studies of land cover change in Ghana have indicated that environmental and social costs from Ghana's gold boom may be higher than previously considered (Schueler et al., 2011). In order to grasp the extent of artisanal mining in Ghana and provide a foundation for informed policy and decision making, it is therefore critical to quantify the extent and rate of gold mining.

Here we use imagery from Landsat 5 TM, Landsat 7 ETM+, and Landsat 8 OLI to identify the extent of land cover conversion to gold mining in Ghana as of 2019. Additionally, we quantified annual changes in industrial and artisanal gold mining in Ghana from 2007 to 2017 to explore the rate of land-use conversions in the country over a 10-year period.

2. Methods

2.1. Study area

This study focuses on Ghana, located in West Africa along the Guinea Coast. Ghana is bordered to the north, east, and west by Burkina Faso, Togo, and Cote d'Ivoire. Ghana has been divided into twelve (12) ecological zones (Ghana's fourth national communication report, 2020). The country experiences a monsoonal climate with two (dry and wet)

dominant seasons (Aryee et al., 2018), which is influenced by the movement of the tropical rain belt (Nkrumah et al., 2014). The northern part of Ghana experiences a unimodal rainfall regime while the southern part experiences a bimodal rainfall. This study focuses on the southern part of Ghana, primarily forested and endowed with natural resources.

A series of tectonic processes in the early Proterozoic Period created a series of gold belts that cover roughly one-sixth of the surface area in Ghana (Lunt et al., 1995). This includes a group of belts containing Birmanian and Tarkwaian gold (Milési et al., 1991). These gold belts largely occur in the southwestern region of the country (Hilson, 2002). The study area was subset to 10,473,030 ha in the southern portion of the country. Historically, this region was defined by forest and agriculture, including Cassava, Cocoa, and Maize (Tappan et al., 2016; Wills, 1962).

2.2. NDVI change detection anomaly

The full workflow of the methodology is depicted in Fig. 1. The full code associated with the methodology is available through Barenblitt et al. (2021a). Satellite imagery for the study area was analyzed using historical Landsat 5 TM, 7 ETM+, and 8 OLI image collections at the nominal spatial resolution, which were accessed and processed through Google Earth Engine (GEE) (Gorelick et al., 2017). Variations between the Landsat 8 and Landsat 5/7 sensor specifications were corrected by using a harmonization process outlined in Roy et al. (2016). Clouds were masked using Landsat's 'pixel_qa' band to eliminate imagery that contained clouds and cloud shadows. The Normalized Difference Vegetation Index (NDVI) was calculated across all pixels using the normalized ratio of red and near-infrared bands for each available satellite image and combined with the existing spectral bands (Rouse et al., 1974). The image collection assembled through this process was used for the anomaly change detection and subsequent random forest classification.

Areas that experienced anomalous vegetation loss from 2005 to 2019 were identified through assembling a Landsat imagery timestack from 2002 to 2005. This timestack established a cloud-free reference period and a baseline NDVI by calculating the median NDVI value for each pixel stack across this 3-year time period. A separate imagery timestack was assembled from 2010 to 2019 to establish an observation period. The reference NDVI image was subtracted from each of the individual NDVI images within the observation period to calculate a cumulative

NDVI loss anomaly between the reference period and the end of the observation period, following a similar approach as (Lagomasino et al., 2019). A mean NDVI change image was derived by dividing the cumulative change anomaly by the number of quality pixels within each pixel stack (e.g., cloud and cloud shadow corrected).

An NDVI loss of 0.15 or more was considered a substantial and prolonged disturbance that could be attributed to conversion from dense vegetation (e.g., forest) to Mining, Urban development, Water, or Other. This threshold was modified based on values outlined in Lagomasino et al. (2019) which yielded results with limited noise and best captured sustained vegetation loss that indicated a significant land cover change. The resulting change detection map (2005 to 2019) calculated from the anomalous NDVI loss was used as the area of interest to later quantify the subsequent land cover conversion types.

2.3. Random forest classification of land cover classes

A contemporary cloud-free composite for the study region was generated using Landsat 8 imagery from 2017 to 2019 using the same pre-processing methods described above. Four land cover classes were used to train the model: Mining, Urban, Water, and Other. Training data for the Mining class were solely represented by artisanal mining regions. However, the model also identified industrial mines, which were later distinguished (see Section 2.4, Large Scale Gold Mines). The Urban class reflected areas of human settlement and the Water class reflected areas of standing water. The Other classification reflected non-forested agriculture, bare soil, and other areas of anomalous vegetation loss not attributable to Mining, Urban, or Water. High-resolution satellite imagery from Google Earth was used to manually select specific regions that corresponded to each of the four land cover types. The selected regions resulted in 60,535 pixels that were incorporated into the training dataset used in a random forest classification model (Breiman, 1996). This included 1072 Mining, 23,757 Other, 2471 Urban, and 33,235 Water pixels. Different machine learning algorithms can result in discrepancies of total area for land cover models, however, random forest models have shown to produce higher user's, or characterization of errors of omission, producer's, or errors of commission, and overall accuracy compared to other approaches (Mondal et al., 2019). The model was run across the entire study region using 100 trees and 5 predictor variables. The resulting land cover classification models were masked to areas identified within the anomalous NDVI loss from 2005 to 2019.

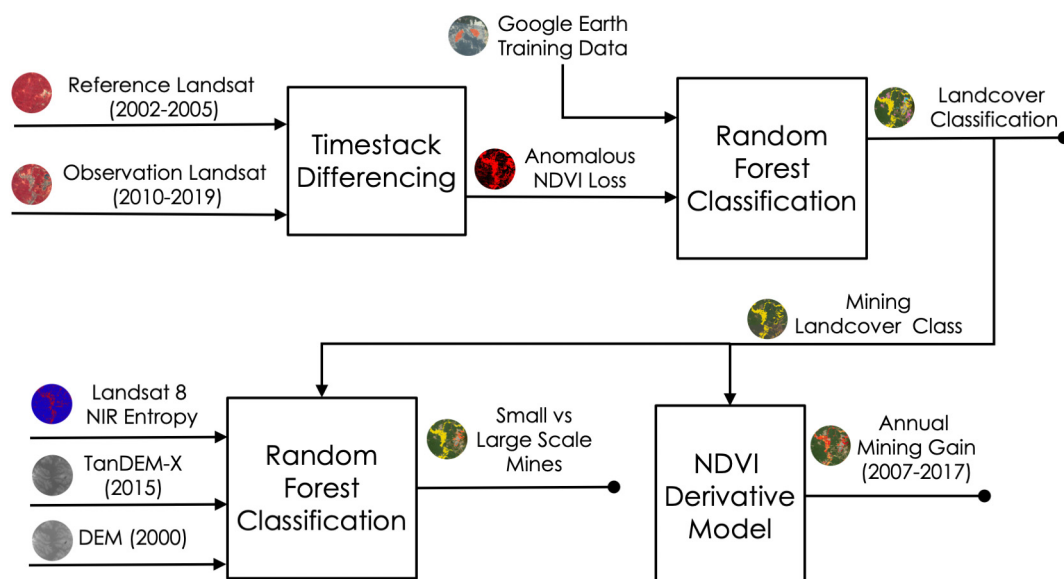


Fig. 1. Workflow of methodology.

2.4. Large scale gold mines

Areas identified as gold mining in the land cover classification model were further differentiated into two categories: large-scale, industrial mining and small-scale, artisanal mining. Industrial mining operations within the study period (2005–2019) were assumed to have a significant change in elevation because of the nature of the mining activities. Based on these assumptions, elevation data from TanDEM-X and the Shuttle Radar Topography Mission (SRTM) was acquired. The Digital Elevation Model (DEM) produced from SRTM in 2000 was subtracted from that produced by TanDEM-X in ~2013 to estimate relative changes in surface elevation. In addition, the Landsat 8 NIR band was used to calculate entropy, or a measure of randomness, and a gray-level co-occurrence matrix (GLCM)-based contrast, which characterizes texture based on co-occurring pixel values. Using a separate, randomly generated validation data (see Section 2.6, Accuracy Assessment and Area Uncertainty) 394 small-scale and 104 industrial mining points were identified through visual interpretation of high-resolution satellite imagery. These data were then used to train a second random forest classification using entropy, GLCM, and the change in DEM as predictors that was confined to the total extent of gold mining from the land cover classification model described above. This classification was then cleaned up through a 10-pixel radius square modal neighborhood filter. The resulting gold mining type model was imported to QGIS 3.10 where it was vectorized using connected pixels and area stats computed for each individual polygon. A threshold size of 1 ha was used in post-processing to separate industrial from artisanal mining.

2.5. Time series analysis

Within GEE, the maximum derivative NDVI, or highest rate of change in NDVI, was calculated across the study area to assemble a time series of gold mining in Ghana and improve understanding of when the majority of mining occurred. To do this, the same preprocessing procedures for the Landsat imagery were applied. Landsat NDVI images were stacked into annual datacubes, whereby the maximum annual NDVI value was

extracted for each pixel and subset to the Mining land-use class defined above in Section 2.3. A 3-year moving average was then applied to the annual NDVI maximums over the entire time period. Next, an annual NDVI derivative model was calculated in order to identify when the maximum loss of NDVI occurred, representing the change in land cover from vegetation to Mining. These results were mosaicked using the year of maximum NDVI loss. We subset the study period to 2007–2017 to focus on years with sufficient cloud-free imagery available to identify annual changes. Results from the model were compared to gold prices reported by the World Gold Council from the same study period. A Spearman's correlation was used to calculate the correlation between gold price and annual mining conversion after a two year lag.

Results from this model were compared to other annual change detection algorithms including LandTrendr (Kennedy et al., 2018) and Continuous Change Detection Classification (CCDC) (Zhu and Woodcock, 2014). LandTrendr is a set of spectral-temporal segmentation algorithms that can be used to detect change across a time series of moderate resolution satellite imagery (Kennedy et al., 2018). It has been previously used to study land cover changes and disturbances (Kennedy et al., 2010). This model was run using a magnitude threshold of 200, duration threshold of 4, and a pre-value of 100. The CCDC algorithm uses harmonic regression and trend models to estimate deviations from gradual changes due to abrupt change (Zhu and Woodcock, 2014). This model was run with 3 minimum observations to flag a change and a chi-square probability threshold of 0.8. Both models were run within the Mining land-use class for direct comparison.

2.6. Accuracy assessment and area uncertainty

To validate the land cover model, randomly stratified points were generated for each cover type within the NDVI anomaly layers, resulting in 484 points for Mining, 535 points for Other, 579 points for Urban, and 523 points for Water. The year of transition to mining was further validated using the same stratified random probability-based sampling approach. A 100 m × 100 m square was centered on each validation point representing a one-hectare block. This one-hectare block was then used

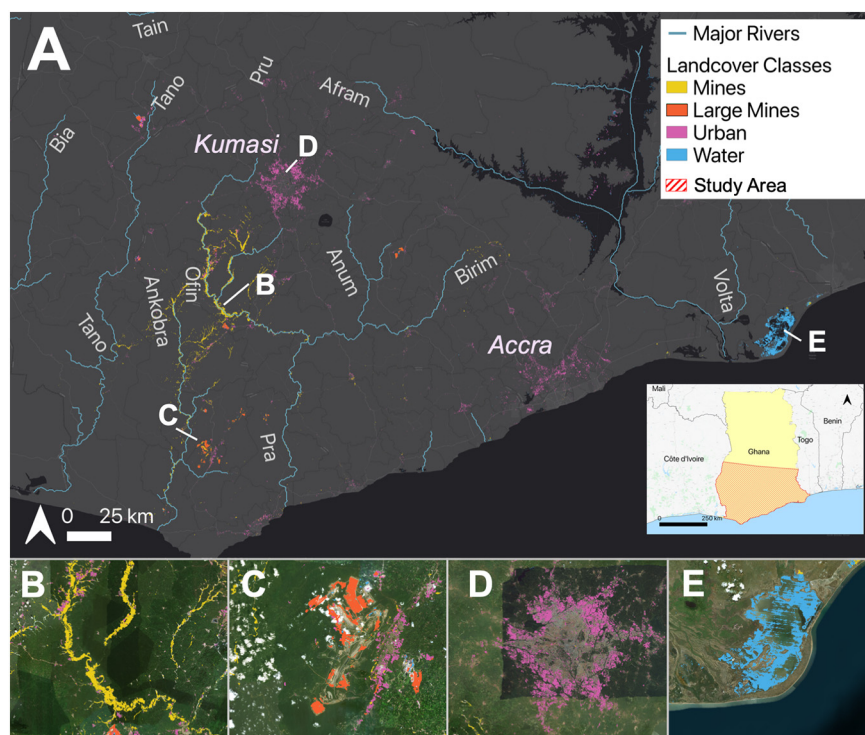


Fig. 2. A) Land cover classification results from Random Forest model; B) example artisanal gold mining region and land cover classification; C) example industrial gold mining region and land cover classification; D) ESRI Satellite imagery of Kumasi and Urban land cover classification; E) classification of Anlo-Keta Lagoon Complex showing conversion to water.

in the visual assessment and interpretation of the land cover class and transition year. The validation of the land cover type and transition year was completed using Google Earth Pro and Collect Earth (Bey et al., 2016).

Google Earth Pro provided high-resolution, but infrequent imagery through time for each of the plots. Collect Earth is an open source software that allows for data collection and further analysis of land coverage using a combination of satellite imagery and NDVI time series graphics from multiple satellite sensors. The combination of high-resolution commercial imagery available in Google Earth Pro and the time series data from Collect Earth allowed for detailed interpretation of shifts in vegetation. The stratified random blocks were imported into Collect Earth with the modeled results removed to provide an unbiased assessment. Two independent analysts validated the land cover classes whereby one analyst validated the Urban and Water classes and the other the Mining and Other classes. Visual interpretations of the current land cover class and year of transition were assessed using the full suite of imagery in Google Earth Pro and Collect Earth. In addition to verifying the land cover and transition year, points with limited data were recorded along with additional comments related to validation. Mining points were also labeled as being within industrial or artisanal gold mining areas.

To assess the accuracy of the land cover classification and transition year, the sample observations were compiled into a confusion matrix, which visualizes an algorithm's performance by comparing actual and predicted values. Metrics such as overall accuracy, Producer's and User's Accuracy, and Commission and Omission Error were calculated. The sample matrix was used to estimate the population matrix based on the best accuracy assessment methods of Oloffson et al. (2014). From this, revised unbiased estimates of the total conversion to each class were calculated.

3. Results

3.1. Model results

Datasets associated with model results are available through Barenblitt et al. (2021a). Between 2005 and 2019, a total of 167,523 ha were estimated as land cover conversion from dense vegetation to Mining, Water, Urban, or Other. Of that, 47,414.2 ha or 28.3% (± 2218 ha) were converted to gold Mining, 48,819.1 ha or 29.1% (± 2073.3 ha) were lost to Urban development, 28,719.2 ha or 17.1% (± 1608.6 ha) were converted to Water, and 42,570.5 ha or 25.4% (± 2660.7 ha) were converted to Other land cover losses (Fig. 2).

Table 1
Confusion Matrix for land cover classifications; total accuracy: 84.2%; adjusted accuracy without other class: 90.4%.

	Validation				Total
	Mining	Urban	Water	Other	
Mining	461	13	10	0	484
Urban	38	466	0	75	579
Model Water	13	0	507	3	523
Other	98	16	69	352	535
Total	610	495	586	430	2121
Producer's Accuracy	75.6%	94.1%	86.5%	81.9%	84.2%
User's Accuracy	95.2%	80.4%	96.9%	65.8%	

Together, conversion to mining and urban accounted for over 57% of total land conversion with nearly identical conversion rates. The accuracy assessment demonstrates that the overall model was 84.2% accurate with the Other class having the lowest user's accuracy at 65.8% and the Mining and Water classes having the highest user's accuracy of 95.2% and 96.9% respectively (Table 1). We re-calculated the matrix using the points from all landcover classes except Other and found the model had an accuracy of 90.4% (Table 1).

Much of the artisanal mining followed rivers, primarily the Ofin and Ankobra Rivers (Fig. 2A). While conversion to Other land cover was scattered across the study area, conversion to mining was concentrated in the Southwest portion of the country, with the majority of loss occurring southwest of Kumasi (Fig. 2B). Of the total 47,414 ha converted to mining, 42,395.4 ha (85.7%) were identified as artisanal mines while 5018.6 ha (14.3%) were identified as industrial mines, primarily associated with 9 industrial mining complexes (Fig. 2C). Conversion to Urban was concentrated around the cities of Kumasi and Accra (Fig. 2D). Conversion to Water was concentrated mainly around the Anlo-Keta Lagoon Complex in the Southeastern region of our study area (Fig. 2E).

3.2. Mining in protected areas

Gold mining occurred primarily across the southwestern portion of the study area, and 723.30 ha of mining occurred across 28 protected areas defined by the World Database on Protected Areas (Tables 2, 1S). The majority of this occurred in Upper Wassaw (466.29 ha or 3.43% of total reported area) and Asenanyo (102.24 ha or 1.52% of total reported area) (Table 2, Fig. 3). Both of these areas are designated by the International Union for Conservation of Nature (IUCN) as Category IV, or habitat/species management areas. Ajenjua Bepo, which is designated as Category VI, or a protected area with sustainable use of natural resources, experienced the highest proportion of area converted to mining. Here, 49.41 ha of mining occurred, which is equivalent to 8.58% of the total reported protected area (Table 2, Fig. 3). Each of these areas is Forest Reserves managed by the Forest Services Division.

3.3. Annual time series

Over the course of the study period, the model indicated that the extent of all mining increased by 4 \times from 8635.5 ha in 2007 to 35,007.5 ha in 2017 at a mean rate of 2637 ha yr⁻¹. Between 2007 and 2017, the model indicated that the majority of mining conversion occurred in 2014 (5785.2 ha) followed by 2015 (5264.9 ha) and 2017 (3444.9 ha) (Figs. 4, 5). The conversion to mining detected during these three years accounted for 50.3% of the total area of mining conversion as of 2017. The annual time series had an overall accuracy of 33.8% for classifying the exact year of conversion. However, within 1 year of actual conversion the time series had an accuracy of 69.4% and within 2 years of actual conversion, an accuracy of 76.1% (Table 2S).

The results of CCDC (Zhu and Woodcock, 2014) and LandTrendr (Kennedy et al., 2018) models for the same years of interest are demonstrated in Fig. 5A–D. An example of annual values of maximum NDVI at the pixel level is compared to annual fitted values calculated by our model and LandTrendr and the CCDC temporal break in Fig. 5A. While our model was more comparable to results from CCDC in terms of overall detected mining extent (28,807.8 ha), LandTrendr was only able to identify annual change for 14,314.9 ha within the areas identified as mining. The CCDC model detected the highest activity in mining in 2013 (5828 ha), 2015 (5142 ha), and 2016 (4422 ha). The differences in the results of this model compared to CCDC and LandTrendr are likely attributable to the differences in model assumptions. CCDC and LandTrendr both use a statistical threshold of NDVI loss to determine the year of conversion, whereas our model assumes that the year of highest NDVI loss rate predicts the year of conversion. The price of gold in USD had a significant correlation with annual mining extent detected by the model used in this study (0.83, $p = 0.005$) (Fig. 5E–F).

Table 2

Mining in protected areas of Ghana, top 5 incidences of mining (FR = forest reserve, FSD = forest services division).

Protected area	Reported area (ha)	Mining area (ha)	Proportion mined (%)	Designation	Managing authority	IUCN category
Upper Wassaw	13,602.37	466.29	3.43	FR	FSD	IV
Asenanyo	6732.79	102.24	1.52	FR	FSD	IV
Ajenjua Bepo	575.87	49.41	8.58	FR	FSD	VI
Tano Suraw	2633.69	5.37	0.2	FR	FSD	VI
Denyau Shelterbelt	1290.99	3.5	0.27	FR	FSD	IV

4. Discussion

4.1. Gold mining extent in Ghana

The results presented here have quantified the extent of gold mining in Ghana and supports previous work that indicated that artisanal mining or *Galamsey* has devastating impacts on terrestrial ecosystems (Espejo et al., 2018; Hilson, 2002; Schueler et al., 2011). Our model quantifies the significant footprint that the accumulation of smaller, artisanal mines leaves on the Ghanaian landscape, especially in comparison to larger, industrial mines. Most notably, while individual industrial mines leave a distinctly deep impression on the landscape, we demonstrate that the cumulative footprint of *Galamsey* was nearly 7 times larger than that of the few industrial mines (Table 1B). While the overall accuracy of the model was 84.2%, the model had a higher accuracy (90.4%) with the omission of the Other class. Additionally, the high user's accuracy of the Mining class (95.2%) is promising for detecting active or non-remediated, dormant mines. To date, few studies have been able to quantify the spatial footprint of gold mining practices (e.g., industrial and *Galamsey*) in Ghana using optical satellite imagery due to the cloudy nature of the region. The nested combination of optical and radar satellite imagery was able to quantify the relative impacts of mining practices. Previously, Owusu-Nimo et al. (2018) used a field-based approach to map gold mining activity in Ghana. However, this work quantified *Galamsey* sites rather than the overall spatial footprint of mining.

Few studies have utilized satellite data to quantify the spatial footprint of *Galamsey* across a large region in Ghana. A recent study by Forkuor et al. (2020) used Sentinel-1 time series to quantify changes in gold mining from 2015 to 2019 within a smaller study area of 9071 km². By comparison, our study area of 104,730 km² was >11× larger, representing a more holistic picture of gold mining across the country. Snapir et al. (2017) focused on a study area comparable to ours (91,400 km²) where gold mining has the potential to impact cocoa farming. This study used an unsupervised classification with UK-DMC2 imagery to quantify the total area of artisanal mining in 2013 and estimated 27,839 ha of gold mining. In comparison, our methodology detects 17,396 ha of mining by 2013, 23,181 ha by 2014, and 28,446 ha by 2015. The Snapir, Simms, and Waine study relied on 3

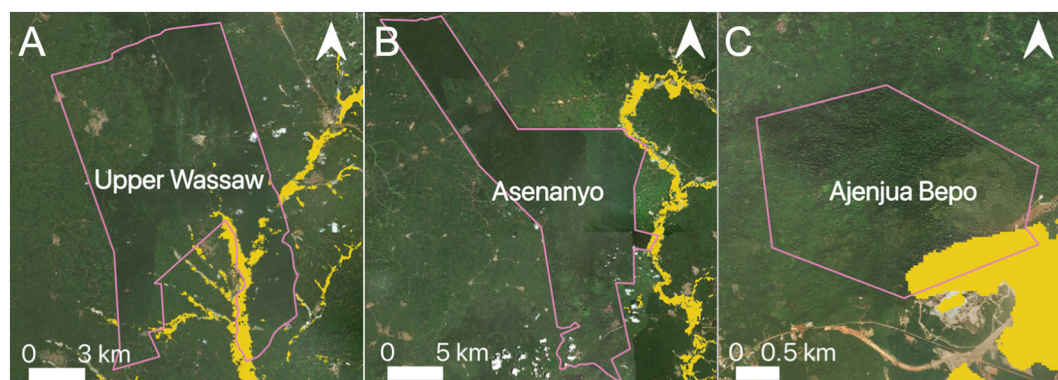
cloud-free images for their analysis, while our methodology mosaicked 3000+ images to create a cloud-free mosaic. Our work also expands upon this previous research by examining a longer time frame (10 years) of land cover change to gold mining in Ghana.

The average rate of conversion to mining (~2600 ha yr⁻¹) in Ghana across the study period is comparable to rates identified in other countries. In particular, previous studies of another active gold mining region, Madre de Dios in the Amazon, have identified an average loss of ~4400 ha yr⁻¹ to gold mining activities since 2000 (Asner and Tupayachi, 2017). Patterns of peak mining activity in Ghana similarly reflected patterns in the Madre de Dios region. In Ghana, >70% of total mining activity occurred between 2009 and 2017 at an average rate of 3188 ha yr⁻¹. Similarly, previous work identified an increase of the average rate of mining in Madre de Dios from less than ~1000 ha yr⁻¹ before 2009 to ~7000 ha yr⁻¹ since 2009 (Espejo et al., 2018).

4.2. Implications of annual analysis

While the land cover classification of mining across the entire study period may include areas where mines have been abandoned, the time series analysis focuses on new mining activity and may serve as a useful tool for identifying patterns in mining activity in the future. According to the model, the most active years of mining during our study period occurred recently, with 50.3% of mining activity between 2007 and 2017 occurring between 2014 and 2017. Increasing demand and value for gold may have contributed to this growth in mining activity within the past decade. Following 2007, gold experienced a dramatic increase in value, jumping from \$695.4/oz. in 2007 to \$1257.2/oz. in 2017 with a peak of \$1669/oz. in 2012 (Owusu et al., 2019). This unprecedented rise in the price of gold correlates with the conversion to mining after a two year lag, demonstrating a strong link between the value of gold and mining activity. A similar correlation between mining activity and gold price was identified in Madre de Dios, however some of the mining activity corresponded with other infrastructure development in the area (Espejo et al., 2018). It is likely that while gold price may explain some patterns in mining activity, other factors, such as proximity to new infrastructure, may also play a role in increased activity.

The peak of gold mining in 2014 and 2015 was followed by a period of reduced mining activity in 2016 and 2017. Forkuor et al. (2020) also

**Fig. 3.** Gold mining encroachment on 3 WDPA's.

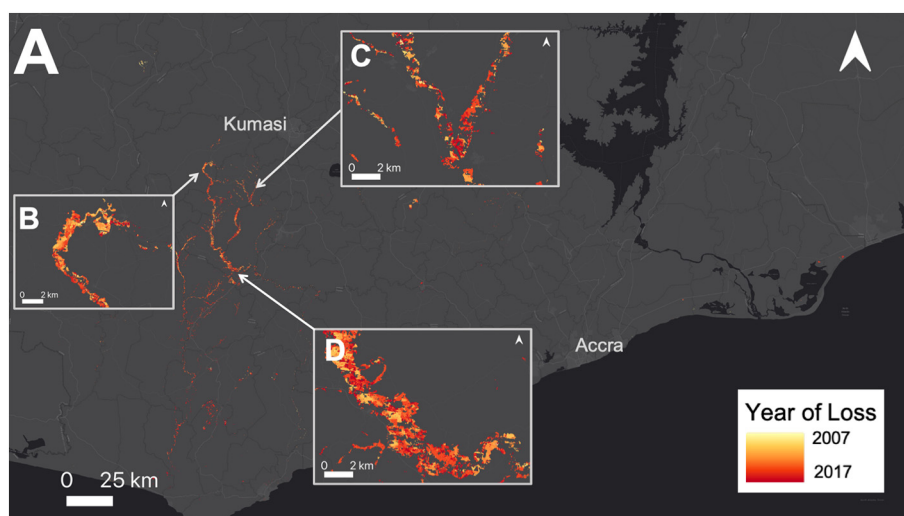


Fig. 4. New mining activity by year from 2007 to 2017.

observed decreased activity between 2016 and 2019 within their study area. This trend is likely related to government efforts to stop artisanal mining. In March 2017, the Ghanaian government created Operation Vanguard, which banned all unlicensed mining activities countrywide and supported this ban using strict enforcement (Hilson, 2017). This followed a significant media campaign centered around the Hg emissions resulting from *Galamsey*. Our analysis indicates that while new mining activity decreased after 2014, 6561.2 ha of new mining activity, or 13.8% of the total calculated mining extent in 2019, occurred from 2016 to 2017 despite the ban on *Galamsey*. Other studies have demonstrated that the two-year ban not only had economic repercussions on local mining communities, especially for women, but was also failed to encourage a shift to sustainable development and required an unsustainable effort from the government and military (Zolnikov, 2020; Tuokuu et al., 2020; Owusu et al., 2019). The ban also failed to address deeper economic problems, such as agricultural poverty, that contribute to the rise of artisanal mining (Owusu et al., 2019; Hilson and Garforth, 2012). Meanwhile, activity in industrial mines ranged from 95.7 ha to 662.4 ha with the highest activity occurring from 2014 to 2017. Unlike artisanal mining, the peak of industrial mining activity occurred in 2017, which may again reflect the focus of the mining ban on artisanal mines.

4.3. Health and food security implications

The resulting map of gold mining also reveals patterns in mining location. Often, artisanal mines appear to be co-located with major rivers, particularly the Ofin and Ankobra Rivers. These mines leave a distinct footprint with a series of ponds along these major rivers. The co-location of many mining operations with major waterways has significant implications for health and water quality in the region, as well as food security. In particular, the amalgamation process to remove gold from sediments can result in heavy metal contamination and have a direct impact on indicators of SDG 3, Good Health and Wellbeing.

Illness and mortality caused by unintentional poisoning is an indicator of the UN's goal to reduce mortality from hazardous chemicals and pollution. Artisanal mining has effects on both the water and air quality in and around mining communities. A 2013 study assessing drinking water in artisanal mining areas in Northern Ghana found turbidity, nitrate, cadmium, total iron, manganese and arsenic levels higher than those recommended by WHO for drinking water (Cobbina, 2013). In Ghana, vapors from amalgamation burning in homes already leads to Hg concentrations exceeding recommended doses (Gyamfi et al.,

2020). Neurological and health problems caused by exposure to mercury are well documented (Crompton et al., 2002; Gibb and O'Leary, 2014; Silbergeld et al., 2005). For children in mining communities, Hg is especially hazardous as studies have identified children living and working nearby mining operations experience ataxia and other neurophysiological degeneration (Bose-O'Reilly et al., 2008).

Additionally, artisanal mines pose a threat to food security in the region. The co-location of artisanal mines with major rivers indicates negative impacts extending beyond deforestation and exposure to Hg, with notable impacts on indicators of SDG 6, Clean Water and Sanitation. Increasing the proportion of the population with access to clean water is critical to meeting the goal of Clean Water for All. Artisanal mines sometimes divert streams and rivers, limiting clean water access for downstream users (Gilbert and Albert, 2016). Additionally, this can cause die-off of fish and affect access to food as well as livelihoods outside of mining (Gilbert and Albert, 2016). Overall food production in artisanal mining regions has also decreased in recent years and the contribution of agriculture to Ghana's Gross Domestic Product (GDP) has declined inversely with mining (Gilbert and Albert, 2016). A case study of food security in Kyebi found a causal relationship between artisanal mines and low food production in mining communities as farmland is lost to mine conversion (Ocansey, 2013). Agricultural poverty and the decreasing viability of small-scale agriculture in a globalized economy appear to contribute to this trend (Hilson and Garforth, 2012). The increased rate of artisanal mining in the past decade therefore holds major implications for the future of agriculture and food security in the country if abandoned mines are not reclaimed.

4.4. Potential impact for protected areas

All three protected areas that experienced the highest conversion to mining are nationally protected areas managed by the Forest Services Division. These protected areas provide habitat for species of conservation concern, including Green-tailed Bristlebill *Bleda eximius* and Tai Forest treefrog *Leptopelis occidentalis* (Center for Applied Biodiversity Science, 2007). While deforestation due to mining is a conservation concern across the region, it is particularly necessary to monitor mining in protected areas, as protected areas contribute to SDG 15 (Life on Earth) and the conservation of important terrestrial ecosystems. Not only does the loss of vegetation result in loss of habitat for wildlife, but previous work has demonstrated that the noise pollution from active artisanal mining sites can negatively affect birds and anurans (Alvarez-Berríos et al., 2016). In addition to their ability to protect

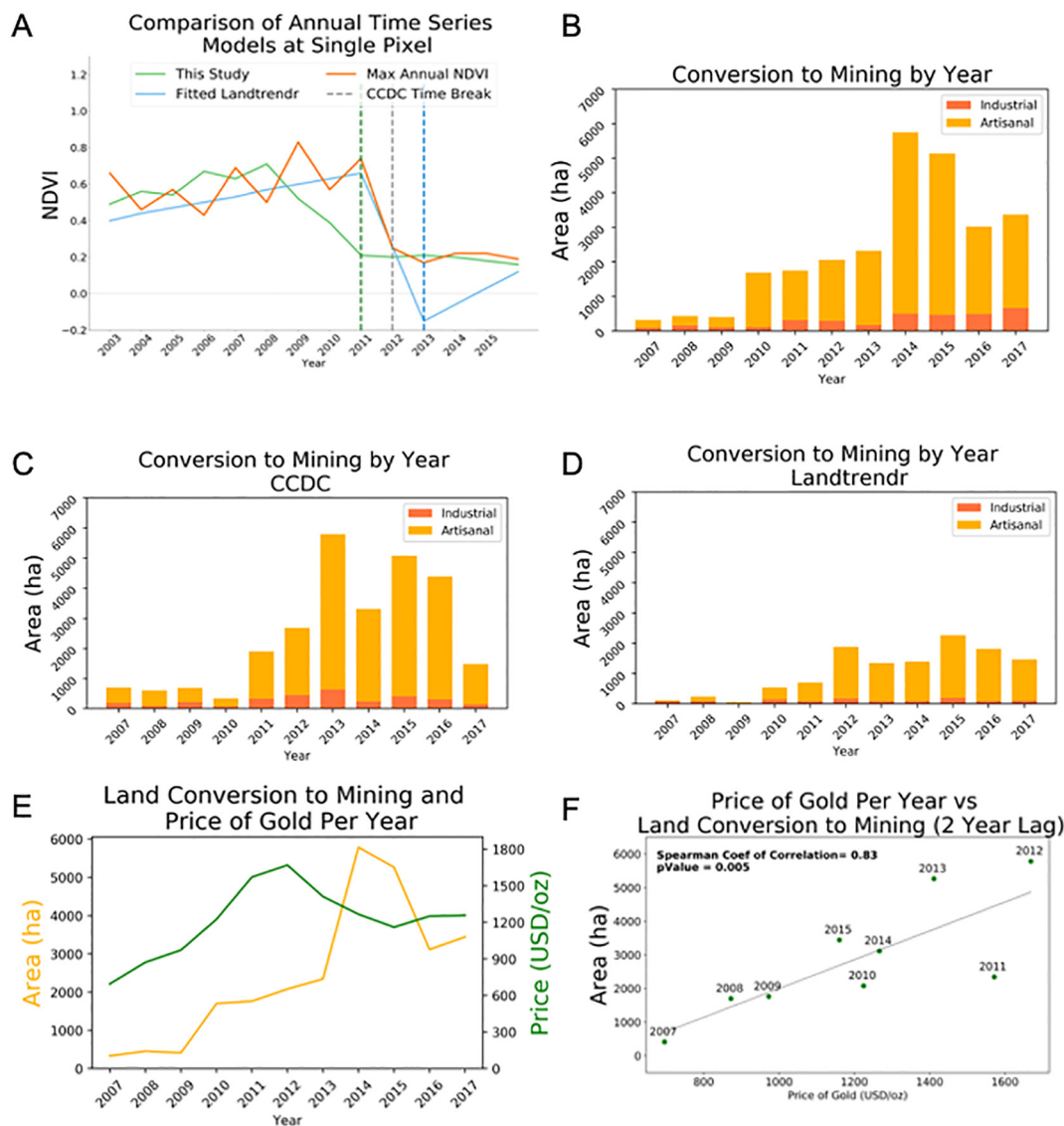


Fig. 5. A) Pixel comparison of time series analysis using Maximum NDVI, LandTendr, Average NDVI Loss, and CCDC; B–D) Comparison of land conversion to mining by year using Maximum Derivative NDVI (This Study), CCDC, and LandTendr. Artisanal mining extent is indicated in yellow. Industrial mining extent is indicated in orange; E) Comparison of land conversion to mining and global price of gold (USD/oz.) from 2007 to 2017, Retrieved September 15, 2020 from www.gold.org/data/gold-price. F) Correlation between price of gold and land conversion to mining two years later. Points indicate the price of gold in the labeled year and area of mining conversion two years later.

biodiversity and species of conservation concern, protected areas in tropical areas also help to lower carbon emissions through reduced deforestation (Bebber and Butt, 2017).

Mining encroachment into protected areas is not unique to Ghana. Protected areas in other countries, including Mongolia and Peru have also experienced encroachment from gold mining (Asner and Tupayachi, 2017; Farrington, 2005). In South America while low mining-related deforestation occurred within strictly protected zones, 32% of total deforestation occurred within the 10 km buffer zone (Espejo et al., 2018). Tracking encroachment of human activity like mining into protected areas is critical. While a small proportion of mining (2.01%) occurs within Ghana's protected areas as of 2019, the proportion of biodiversity hotspots within protected areas is one of several indicators supporting SDG 15 and conservation of life on land. Further encroachment in the future could limit the ability of protected areas to meet local and global conservation goals. The monitoring of mining in these protected areas is therefore pivotal to the preservation of both ecological and economic resources.

4.5. Model limitations

It should be noted that our classification model necessarily targets surface mining activities, rather than subterranean operations. While the user accuracy for the Mining model was high (95.2%), the Producer Accuracy was only 75.6%. Misclassified Mining areas were most often classified as Urban or Other by the model. Mining areas often contain areas of bare soil, which have a high reflectance. Highly reflective surfaces are also largely indicative of urban areas. Additionally, Mining points that were classified as Other by the model sometimes occurred in areas where vegetation was mixed in with mining ponds, making them more difficult to classify. The annual classification is a preliminary step in improving the capability of remote sensing to identify annual mining conversion. While exact predictions of annual conversion to mining require further refinement, the model more accurately predicted the year of conversion within 1 or 2 years of user defined conversion. Additionally, results of this model appear to agree with results from CCDC, and identify peak mining activity after 2009, which is consistent with

mining trends in other studies (Asner and Tupayachi, 2017; Espejo et al., 2018). In general, the model most commonly misclassified conversion as earlier than the actual year conversion. The limited number of available cloud-free images prior to 2012 likely exaggerates the signal for loss in earlier years of the study period and biases the model. Additionally, our model provides satellite-based estimates of artisanal gold mining. However, marginalized rural communities and local stakeholders should be involved in mapping efforts to help relieve potential tensions with “top-down” monitoring efforts as discussed in prior studies of GIS monitoring (Spiegel et al., 2012).

5. Conclusion

This study quantified the spatial and temporal variability in annual vegetation loss due to artisanal mining in southern Ghana, allowing us to identify where distinct patterns of mining and better quantify the footprint of artisanal mining in the country. In a region where spatial studies of artisanal mining are scarce due to limitations in optical imagery coverage, our findings support the ability for Ghanaian agencies to monitor *Galamsey* operations within the country. Our findings suggest that artisanal mining can have devastating impacts on terrestrial ecosystems, where the cumulative footprint can be larger than that of industrial mining. The vegetation loss and presumptive mercury pollution along rivers and in protected areas has negative implications for human and ecosystem health. While this work focused on land conversion, future work in this area could aim to estimate the sedimentation and mercury pollution due to artisanal mining. A continuation of land conversion research could assess the impacts to other classes, such as agriculture, to complete the understanding of food security impacts. Future iterations of the annual classification could be improved through fusion with other satellites, such as the Sentinel series and annual ALOS data, and fine tuning of the algorithm. As more imagery becomes available, annual impacts can also be updated and improved to enable detection of spatial patterns in mining and predict vulnerability to future conversion.

Supplementary data to this article can be found online at <https://doi.org/10.1016/j.scitotenv.2021.146644>.

Funding

This research was funded by the NASA Ecological Forecasting / Sustaining Living Systems in a Time of Climate Variability and Change Program [grant number 80NSSC19K0205].

CRediT authorship contribution statement

Abigail Barenblitt: Writing – original draft, Investigation, Visualization. **Amanda Payton:** Conceptualization, Methodology, Validation, Formal analysis. **David Lagomasino:** Supervision, Writing – review & editing, Funding acquisition. **Lola Fatoyinbo:** Conceptualization, Resources, Funding acquisition, Supervision. **Kofi Asare:** Writing – review & editing, Resources. **Kenneth Aidoo:** Writing – review & editing, Resources. **Hugo Pigott:** Writing – review & editing, Project administration. **Charles Kofi Som:** Writing – review & editing, Project administration. **Laurent Smeets:** Writing – review & editing, Project administration. **Omar Seidu:** Writing – review & editing, Project administration. **Danielle Wood:** Conceptualization, Writing – review & editing, Funding acquisition, Project administration, Supervision.

Declaration of competing interest

The authors declare that they have no known competing financial interests or personal relationships that could have appeared to influence the work reported in this paper.

Acknowledgements

We would like to thank Celio de Sousa for providing edits on the manuscript. We also thank Dr. Foster Mensah and the team at the Center for Remote Sensing and GIS at the University of Ghana for reviewing the methods presented in this manuscript. This work was conducted at the National Aeronautics and Space Administration Goddard Space Flight Center. This project was funded by The Ecological Forecasting Team at the NASA Applied Sciences Program [grant number 80NSSC19K0205] within NASA's Earth Science Division. Team members in the collaborative project under the grant represent Massachusetts Institute of Technology, Goddard Space Flight Center and East Carolina University.

References

- Afriyie, K., Ganle, J.K., Adomako, J.A.A., 2016. The good in evil: a discourse analysis of the *galamsey* industry in Ghana. *Oxf. Dev. Stud.* 44 (4), 493–508. <https://doi.org/10.1080/13600818.2016.1217984>.
- Alonzo, Michael, Van Den Hoek, Jamon, Ahmed, Nabil, 2016. Capturing coupled riparian and coastal disturbance from industrial mining using cloud-resilient satellite time series analysis. *Sci. Rep.* 6 (October), 1–12. <https://doi.org/10.1038/srep35129>.
- Alvarez-Berrios, Nora, et al., 2016. Impacts of small-scale gold mining on birds and anurans near the Tambopata Natural Reserve, Peru, assessed using passive acoustic monitoring. *Tropical Conservation Science* 9 (2), 832–851. <https://doi.org/10.1177/194008291600900216>.
- Anenberg, S. C., Bindl, M., Brauer, M., Castillo, J. J., Cavalieri, S., Duncan, B. N., et al. (2020). Using satellites to track indicators of global air pollution and climate change impacts: Lessons learned from a NASA-supported science-stakeholder collaborative. *GeoHealth*, 4, e2020GH000270. DOI: <https://doi.org/10.1029/2020GH000270>.
- Aryee, J.N.A., Amekudzi, L.K., Quansah, E., Klutse, N.A.B., Atiah, W.A., Yorke, C., 2018. Development of high spatial resolution rainfall data for Ghana: development of high spatial resolution rainfall data for Ghana. *Int. J. Climatol.* 38 (3), 1201–1215. <https://doi.org/10.1002/joc.5238>.
- Asner, G.P., Tupayachi, R., 2017. Accelerated losses of protected forests from gold mining in the Peruvian Amazon. *Environ. Res. Lett.* 12 (9). <https://doi.org/10.1088/1748-9326/aa7dab>.
- Authority on Gold (World Gold Council). Available online: <https://www.gold.org/> (accessed on September 15, 2020).
- Bebber, Daniel P., Butt, Nathalie, 2017. Tropical protected areas reduced deforestation carbon emissions by one third from 2000–2012. *Sci. Rep.* 7 (1). <https://doi.org/10.1038/s41598-017-14467-w>.
- Bey, Adia, et al., 2016. Collect earth: land use and land cover assessment through augmented visual interpretation. *Remote Sens.* 8 (10). <https://doi.org/10.3390/rs8100807>.
- Bose-O'Reilly, Stephan, et al., 2008. Mercury as a serious health hazard for children in gold mining areas. *Environ. Res.* 107 (1), 89–97. <https://doi.org/10.1016/j.envres.2008.01.009>.
- Breiman, L., 1996. Bagging predictors. *Mach. Learn.* 24, 123–140. <https://doi.org/10.1007/BF00586555>.
- Barenblitt, A., Payton, A., Lagomasino, D., 2021a. “Ghana Annual Conversion to Gold Mining 2007–2017 and Total Conversion up to 2019”, Mendeley Data, V2. <https://doi.org/10.17632/s4rfckr39.2>.
- Barenblitt, A., Payton, A., Lagomasino, D., 2021b. Ghana Artisanal Mining. Github, V1 <https://doi.org/10.5281/zenodo.4602363>.
- Cabeza, M., Terraube, J., Burgas, D., Temba, E. M., & Rakoarijaana, M. 2019. Gold is not green: artisanal gold mining threatens Ranomafana National Park's biodiversity. In *Animal Conservation* (Vol. 22, Issue 5, pp. 417–419). Blackwell Publishing Ltd. DOI: <https://doi.org/10.1111/acv.12475>.
- Center for Applied Biodiversity Science. 2007. A rapid biodiversity assessment of the Ajenjua Bepo and Mamnag River Forest Reserves, Ghana. (BioOne.) Arlington, VA: Conservation International, Center for Applied Biodiversity Science.
- Cobbina, S. J. 2013. “Small Scale Gold Mining and Heavy Metal Pollution: Assessment of Drinking Water Sources in Datuku In the Talensi-Nabdam District.” *INTERNATIONAL JOURNAL OF SCIENTIFIC & TECHNOLOGY RESEARCH* 2(1). www.ijstr.org.
- Crompton, Peter, et al., 2002. Assessment of mercury exposure and malaria in a Brazilian Amazon Riverine Community. *Environ. Res.* 90 (2), 69–75. <https://doi.org/10.1006/enrs.2002.4358>.
- Csillik, Ovidiu, Asner, Gregory P., 2020. Aboveground carbon emissions from gold mining in the Peruvian Amazon. *Environ. Res. Lett.* 15 (1), 014006. <https://doi.org/10.1088/1748-9326/ab639c>.
- Diringer, Sarah E., et al., 2019. Deforestation due to artisanal and small-scale gold mining exacerbates soil and mercury mobilization in Madre de Dios, Peru. *Environ. Sci. Technol.* <https://doi.org/10.1021/acs.est.9b06620>.
- Esdaile, L. J., & Chalker, J. M. 2018. The Mercury Problem in Artisanal and Small-Scale Gold Mining. In *Chemistry - A European Journal* (Vol. 24, Issue 27, pp. 6905–6916). Wiley-VCH Verlag. DOI: <https://doi.org/10.1002/chem.201704840>.
- Eshun, P.A., Okyere, E., 2017. Assessment of the challenges in policy implementation in the small scale gold mining sector in Ghana-a case study. *Ghana Mining Journal* 17 (1), 54–63. <https://doi.org/10.4314/gm.v17i1.6>.

- Espejo, Jorge Caballero, et al., 2018. Deforestation and Forest degradation due to gold Mining in the Peruvian Amazon: a 34-year perspective. *Remote Sens.* 10 (12), 1–17. <https://doi.org/10.3390/rs10121903>.
- Farrington, John D., 2005. The impact of mining activities on Mongolia's protected areas: a status report with policy recommendations. *Integr. Environ. Assess. Manag.* 1 (3), 283–289. <https://doi.org/10.1897/2004-008R.1>.
- Forkuor, Gerald, Ullmann, Tobias, Griesbeck, Mario, 2020. Mapping and monitoring small-scale mining activities in Ghana using sentinel-1 time series (2015–2019). *Remote Sens.* 12 (6). <https://doi.org/10.3390/rs12060911>.
- Gibb, Herman, O'Leary, Keri Grace, 2014. Mercury exposure and health impacts among individuals in the artisanal and small-scale gold mining community: a comprehensive review. *Environ. Health Perspect.* 122 (7), 667–672. <https://doi.org/10.1289/ehp.1307864>.
- Gilbert, Danyo, and Osei-Bonsu Albert. 2016. "Illegal Small-Scale Gold Mining in Ghana: A Threat to Food Security." *Journal of Food Security* 4(5): 112–19. DOI: 10.12691/jfs-4-5-2.
- Gorelick, Noel, et al., 2017. Google earth engine: planetary-scale geospatial analysis for everyone. *Remote Sens. Environ.* 202, 18–27. <https://doi.org/10.1016/j.rse.2017.06.031>.
- Government of Ghana. 2019. Voluntary National Review (VNR) Report on the Implementation of the 2030 Agenda for Sustainable Development.
- Gyamfi, Opoku, et al., 2020. Human health risk assessment of exposure to indoor mercury vapour in a Ghanaian artisanal small-scale gold mining community. *Chemosphere* 241 (October). <https://doi.org/10.1016/j.chemosphere.2019.125014>.
- Hakimdar, Raha, et al., 2020. Monitoring water-related ecosystems with earth observation data in support of sustainable development goal (SDG) 6 reporting. *Remote Sens.* 12 (10). <https://doi.org/10.3390/rs12101634>.
- Hilson, Gavin, 2002. The environmental impact of small-scale gold mining in Ghana: identifying problems and possible solutions. *Geogr. J.* 168 (1), 57–72. <https://doi.org/10.1111/1475-4959.00038>.
- Hilson, Gavin, 2017. "Shootings and Burning Excavators: Some Rapid Reflections on the Government of Ghana's Handling of the Informal Galamsey Mining 'Menace'." *Resources Policy* 54: 109–16. DOI: <https://doi.org/10.1016/j.resourpol.2017.09.009>.
- Hilson, G., Garforth, C., 2012. "Agricultural poverty" and the expansion of artisanal mining in sub-Saharan Africa: experiences from Southwest Mali and Southeast Ghana. *Popul. Res. Policy Rev.* 31 (3), 435–464. <https://doi.org/10.1007/s11113-012-9229-6>.
- Isidro, Celso M., McIntyre, Neil, Lechner, Alex M., Callow, Ian, 2017. Applicability of earth observation for identifying small-scale mining footprints in a wet tropical region. *Remote Sens.* 9 (9). <https://doi.org/10.3390/rs9090945>.
- Kennedy, Robert E., Yang, Zhiqiang, Cohen, Warren B., 2010. Detecting trends in Forest disturbance and recovery using yearly Landsat time series: 1. LandTrendr - temporal segmentation algorithms. *Remote Sens. Environ.* 114 (12), 2897–2910. <https://doi.org/10.1016/j.rse.2010.07.008>.
- Kennedy, Robert E., et al., 2018. Implementation of the LandTrendr algorithm on Google earth engine. *Remote Sens.* 10 (5), 1–10. <https://doi.org/10.3390/rs10050691>.
- Lagomasino, David, et al., 2019. Measuring mangrove carbon loss and gain in deltas. *Environ. Res. Lett.* 14 (2). <https://doi.org/10.1088/1748-9326/aaf0de>.
- Lobo, F.L., Costa, M.P.F., Novo, E.M.L.M., 2015. Time-series analysis of Landsat-MSS/TM/OLI images over Amazonian waters impacted by gold mining activities. *Remote Sens. Environ.* 157, 170–184. <https://doi.org/10.1016/j.rse.2014.04.030>.
- Lobo, Felipe de Lucia, et al., 2018. Mapping mining areas in the Brazilian Amazon using MSI/sentinel-2 imagery (2017). *Remote Sens.* 10 (8). <https://doi.org/10.3390/rs10081178>.
- Lunt, D.J., Kirby, E., Ritchie, I.C., 1995. *Design of Gold Projects in Ghana in African Mining '95*. Institution of Mining and Metallurgy, London, pp. 333–352.
- Marceau, Danielle J., Hay, G.J., 1999. Remote sensing contributions to the scale issue. *Can. J. Remote. Sens.* 25 (4), 357–366. <https://doi.org/10.1080/07038992.1999.10874735>.
- Martinez, Gerardo, et al., 2018. Mercury contamination in riverine sediments and fish associated with artisanal and small-scale gold mining in Madre de Dios, Peru. *Int. J. Environ. Res. Public Health* 15 (8). <https://doi.org/10.3390/ijerph15081584>.
- Milési, J.P., Ledru, P., Ankrah, P., Johan, V., Marcoux, E., Vinchon, C., 1991. The metallogenic relationship between Birimian and Tarkwaian gold deposits in Ghana. *Mineral. Deposita* 26 (3), 228–238.
- Mondal, Pinki, Xue, Liu, Fatoyinbo, Temilola E., Lagomasino, David, 2019. Evaluating combinations of Sentinel-2 data and machine-learning algorithms for mangrove mapping in West Africa. *Remote Sens.* 11 (24). <https://doi.org/10.3390/rs11242928>.
- Nkrumah, F., Klutse, N.A.B., Aduko, D.C., Owusu, K., Quagraine, K.A., Owusu, A., Gutowski, W., 2014. Rainfall variability over Ghana: model versus rain gauge observation. *Int. J. Geosci.* 05 (07), 673–683. <https://doi.org/10.4236/ijg.2014.57060>.
- Obodai, Josephine, Kwaku Amaning Adjei, Samuel Nii Odai, and Mawuli Lumor. 2019. "Land Use/Land Cover Dynamics Using Landsat Data in a Gold Mining Basin-the Ankobra, Ghana." *Remote Sensing Applications: Society and Environment* 13(October 2018): 247–56. DOI: <https://doi.org/10.1016/j.rsase.2018.10.007>.
- Ocansey, T.I., 2013. *Mining Impacts on Agricultural Lands and Food Security: Case Study of Towns in and around Kyebi in the Eastern Region of Ghana*. Turku University of Applied Sciences, Bachelor Thesis.
- Oloffson, P., Foody, G.M., Herold, M., et al., 2014. Good practices for estimating area and assessing accuracy of land change. *Remote Sens. Environ.* 148, 42–57. <https://doi.org/10.1016/j.rse.2014.02.015>.
- Owusu, Obed, Bansah, Kenneth Joseph, Mensah, Albert Kobina, 2019. 'Small in size, but big in impact': socio-environmental reforms for sustainable artisanal and small-scale mining. *Journal of Sustainable Mining* 18 (1), 38–44. <https://doi.org/10.1016/j.jsm.2019.02.001>.
- Owusu-Nimo, F., et al., 2018. Spatial distribution patterns of illegal artisanal small scale gold mining (Galamsey) operations in Ghana: a focus on the Western Region. *Western Region. Heliyon* 4, 534. <https://doi.org/10.1016/j.heliyon.2018.e00534>.
- Rouse, J.W., Hass, R.H., Schell, J.A., Deering, D.W., Harlan, J.C., 1974. *Monitoring the Vernal Advancement and Retrogradation (Greenwave Effect) of Natural Vegetation. NASA/GSFC Type III Final Report, NASA/GSFC, Greenbelt, MD*.
- Roy, D.P., et al., 2016. Characterization of Landsat-7 to Landsat-8 reflective wavelength and normalized difference vegetation index continuity. *Remote Sens. Environ.* 185, 57–70. <https://doi.org/10.1016/j.rse.2015.12.024>.
- Schueler, Vivian, Kuemmerle, Tobias, Schröder, Hilmar, 2011. Impacts of surface gold mining on land use systems in Western Ghana. *Ambio* 40 (5), 528–539. <https://doi.org/10.1007/s13280-011-0141-9>.
- Silbergeld, Ellen K, Ines A Silva, and Jennifer F Nyland. 2005. "Mercury and Autoimmunity: Implications for Occupational and Environmental Health." *Toxicology and Applied Pharmacology* 207(2, Supplement): 282–92. DOI: 0.1016/j.taap.2004.11.035.
- Snapp, B., Simms, D.M., Waine, T.W., 2017. Mapping the expansion of Galamsey gold mines in the cocoa growing area of Ghana using optical remote sensing. *Int. J. Appl. Earth Obs. Geoinf.* 58, 225–233. <https://doi.org/10.1016/j.jag.2017.02.009>.
- Spiegel, S.J., Ribeiro, C.A.A.S., Sousa, R., Veiga, M.M., 2012. Mapping spaces of environmental dispute: Gis, mining, and surveillance in the Amazon. *Ann. Assoc. Am. Geogr.* 102 (2), 320–349. <https://doi.org/10.1080/00045608.2011.641861>.
- Swenson, Jennifer J., Carter, Catherine E., Domec, Jean Christophe, Delgado, Cesar I., 2011. Gold mining in the Peruvian Amazon: global prices, deforestation, and mercury imports. *PLoS One* 6 (4). <https://doi.org/10.1371/journal.pone.0018875>.
- Tappan, G.G., Cushing, W.M., Cotillon, S.E., Mathis, M.L., Hutchinson, J.A., Herrmann, S.M., Dalsted, K.J., 2016. West Africa Land Use Land Cover Time. U.S. Geological Survey data release, Series <https://doi.org/10.5066/F73N21JF>.
- Tuokuu, F.X., Idemudia, U., Bawelle, E.B.G., Baguri Sumani, J.B., 2020. Criminalization of "galamsey" and livelihoods in Ghana: limits and consequences. *Nat. Res. Forum* 44 (1), 52–65. <https://doi.org/10.1111/1477-8947.12189>.
- UN Environment, 2019. *Global Mercury Assessment 2018*. UN Environment Programme, Chemicals and Health Branch Geneva, Switzerland.
- Wills, J.B., 1962. *Agriculture and land use in Ghana*. Oxford University Press, London.
- Zhu, Zhe, Woodcock, Curtis E., 2014. Continuous change detection and classification of land cover using all available Landsat data. *Remote Sens. Environ.* 144, 152–171. <https://doi.org/10.1016/j.rse.2014.01.011>.
- Zolnikov, T.R., 2020. Effects of the government's ban in Ghana on women in artisanal and small-scale gold mining. *Resources Policy* 65. <https://doi.org/10.1016/j.resourpol.2019.101561>.